NIH Public Access
Author Manuscript
Biosens Bioelectron. Author manuscript; available in PMC 2011 May 15.

Published in final edited form as:
Biosens Bioelectron. 2010 May 15; 25(9): 2107–2114. doi:10.1016/j.bios.2010.02.013.

Nonlinear dielectric spectroscopy for label-free detection of respiratory activity in whole cells

G.T. "Skip" Mercier[1,2], **Akilan Palanisami**[1], and **John H. Miller Jr.**[1]

[1]Department of Physics and Texas Center for Superconductivity, University of Houston, Houston, TX

Abstract

We report on a novel electromagnetic biosensing technique for detecting respiratory activity in whole cells suspended in aqueous solution. Application of a pure sinusoidal voltage between two outer electrodes applies an oscillatory electric field to the aqueous cell suspension at frequencies in the range of one to several kHz. The fundamental and higher order harmonic responses are measured across two inner electrodes using a dynamic signal analyzer. Aqueous suspensions of S. *cerevisiae* (budding yeast), with both active and inactive mitochondrial electron transport (respiratory) chains are employed for this study. We find that the measured third harmonic for certain frequency ranges shows significant temporal changes in actively respiring yeast, while little significant changes are observed in yeast with suppressed respiratory activity, i.e. mutant yeast strains or yeast in the presence of respiratory inhibitors. The method holds potential for further development to detect respiratory activity in live tissue *in vitro* and perhaps *in vivo* for clinical applications.

Keywords

mitochondria; biosensing; respiratory activity; harmonic analysis; nonlinear dielectric spectroscopy

1. INTRODUCTION

The role of mitochondrial dysfunction is increasingly being recognized in aging, cardiovascular disease, cancer, and metabolic diseases, such as type-2 diabetes, primarily associated with obesity. The World Health Organization estimates that the number of obese and overweight people globally now exceeds the number who are malnourished. This epidemic has several potential negative health consequences ranging from type-2 diabetes to heart disease. In addition, increased visceral fat predisposes obese and overweight individuals to metabolic syndrome, characterized by increased free fatty acids and the subsequent manifestation of insulin resistance (Bergman *et al.*, 2007).

Deficits in the number, size, and function of mitochondria in a wide range of tissues have been implicated in obesity (Ritov *et al.*, 2005) and type 2 diabetes (Lowell and Shulman, 2005). Mitochondrial dysfunction has been hypothesized to be central to insulin resistance and hyperglycemia in type 2 diabetes (Lowell and Shulman, 2005). Mitochondria are also

© 2010 Elsevier B.V. All rights reserved.

[2]Corresponding author, 202 Houston Science Center, Houston, Texas 77204-5002, 713-743-7312, Fax: 713-743-8201, gmercier@uh.edu.

Publisher's Disclaimer: This is a PDF file of an unedited manuscript that has been accepted for publication. As a service to our customers we are providing this early version of the manuscript. The manuscript will undergo copyediting, typesetting, and review of the resulting proof before it is published in its final citable form. Please note that during the production process errors may be discovered which could affect the content, and all legal disclaimers that apply to the journal pertain.

NIH-PA Author Manuscript
NIH-PA Author Manuscript
NIH-PA Author Manuscript

NIH-PA Author Manuscript
NIH-PA Author Manuscript
NIH-PA Author Manuscript

associated with altered bioenergetics that can result in heart failure in the context of insulin resistance and nutrient excess (Ingwall, 2009; Neubauer, 2007).

Given recent literature supporting mitochondria as the harbingers of metabolic disorders low-cost, noninvasive methods of detection of mitochondrial function in at-risk individuals are critical for the future of public health. Mitochondria are inherently electromagnetic organelles: they sustain about 140 mV (Alberts *et al.*, 2002) of membrane potential and ongoing electron flux. Therefore it may be possible to use electromagnetic sensors of dielectric phenomena to evaluate metabolic activity. In fact, Astumian and Robertson (1989) gave a theoretical analysis of how membrane proteins can give rise to nonlinear phenomena in the presence of an oscillating electrical field, and Woodward and Kell (1990, 1991a, 1991b) measured nonlinear behavior in the outer membranes of microbial suspensions using an applied sinusoidal field.

Conventionally, mitochondrial defects are determined by measuring the respiratory control ratio: patient cell samples are taken, mitochondria are isolated, and respiration is measured using substrates and an oxygen sensor. This technique is highly laborious and thus impractical on a wide scale. Electromagnetic sensors could eliminate the mitochondrial isolation step and possibly even provide for *in situ* measurements using a similar electrode arrangement as in electrocardiography.

In this communication, we report dynamic nonlinear phenomena in yeast that correlate with respiratory capacity and rate, and corroborated by oxygen consumption measurements, using an experimental apparatus with two outer driving and two inner sensing electrodes. We also find that yeast mutants lacking functional mitochondria and the associated respiratory activity display static nonlinear responses consistent with the absence of respiration. Similar results were obtained using mitochondrial inhibitors as a means to retard or halt respiratory activity. The results suggest that specific characteristics of an excitatory electrical field coupled with nonlinear harmonic analysis could be used to probe and evaluate the function of mitochondria.

2. EXPERIMENTAL

2.1 Yeast strains, media, buffers, and reagents

Respiration competent strain D273-10B (Sherman, 1963) and deficient strain DS400/A12 (Nobrega and Tzagoloff, 1980) were purchased from American Type Culture Collection (ATCC, Manassas, VA). Respiratory-deficient yeast knock-out mutants YBL080C, YBL099W, and YEL024W, generated by the *Saccharomyces* Genome Deletion Project, were also obtained from ATCC. Yeast cellular concentration was calculated by multiplying the optical density at 600 nm with the empirical factor of 10^6 cells/ml per 0.1. All strains were grown in YPD medium (10 g yeast extract, 20 g Bacto peptone, and 20 g glucose per liter) and washed twice with phosphate-buffered saline (PBS, 80 g NaCl, 2 g KCl, 14.4 g Na_2HPO_4, and 2.4 g KH2PO4 per liter). Respiration buffer was PBS with 100 mM glucose. Mitochondrial inhibitors included potassium cyanide, myxothiazol, and mixed antimycins purchased from Sigma-Aldrich (St. Louis, MO).

2.2 Oxygen consumption measurements

Oxygen consumption was recorded using a Strathkelvin (North Lanarkshire, Scotland) Clark-type polarographic electrode relative to 100% saturation of buffer at room temperature. An FEP membrane was used with stirring performed by a small Teflon stir bar to enable fast measurement response. Before each experiment, buffers were vigorously shaken to generate saturated solutions. For oxygen-depleted experiments, a vacuum was pulled overnight on the solutions before use.

NIH-PA Author Manuscript

NIH-PA Author Manuscript

NIH-PA Author Manuscript

2.3 Electrode configuration, voltage source, and data acquisition

A tetrapolar electrode configuration was constructed using four, 0.01-cm diameter gold wires (99.99% pure) spaced 2 mm apart mounted on a glass microscope slide with epoxy adhesive at either end. The plus and minus BNC outputs of a Stanford Research Systems (SRS, Sunnyvale, CA) DS-360 Ultra Low Distortion Function Generator were connected to the outer two gold wires. The inner two wires were connected to an SRS SR785 Dynamic Signal Analyzer, also known as a spectrum analyzer (Fig. 1). The SR785 was set to use a 262 kHz sampling rate and duration of 7.8 ms for each time record. For all measurements, the FFT function (with 8 averages of the exponential/continuous type) was used to transform all measurements into the frequency domain collected as a fundamental and series of harmonic frequencies and amplitudes. Multiple driving frequencies (1 kHz to 9 kHz) were tested at each time point by setting the function generator, setting the driving amplitude to ±2 V (peak-to-peak), taking harmonic amplitude values, turning off the function generator output, and repeating for the next frequency. This frequency sweeping technique and all other measurements were aided by virtual instruments in National Instruments (Austin, TX) LabVIEW software.

2.4 Data Analysis and Statistics

All experiments were carried out in triplicate measurements and the results reported represent the means with error bars representing the standard deviations. Where indicated, statistical significance was measured using a paired Student's t test with a P value being less than 0.05. Graphing and statistical analysis was performed with GraphPad Prism software and Microsoft Excel.

3. RESULTS

Budding yeast (*Saccharomyces cerevisiae*) was selected as a model for studying nonlinear dielectric spectroscopy of metabolic processes. Specifically, the D273-10B strain was chosen for its normal cytochrome content and resistance to glucose repression (Altmann *et al.*, 2007; Sherman, 1963; Sherman and Slonimski, 1964). These eukaryotes are ideal since they can be quickly grown to high titers and much of their mitochondrial biology is known. Additionally, increased growth rates lead to high metabolic rates, allowing for real-time observations of time-varying harmonic fluctuations.

A four-probe non-linear dielectric spectrometer was constructed as in (Woodward and Kell, 1990) with various modifications. The gold wires were secured by gluing the ends of four gold wires onto a small glass slide to prevent lateral movement during mixing of the cellular suspension. Previous measurements using wires without the glass secured from either end only produced data that was highly variable, measuring large changes when small perturbations in the surrounding environment were present. The two outer wires were connected to an ultra-low distortion function generator and the two inner wires were connected to the spectrum analyzer (Fig. 1). This setup excluded the use of a reference cell since measurements on respiring microorganisms are inherently time-dependent processes. Thus, only changes in harmonics referenced from an initial state must be considered instead of absolute harmonics of a resting suspension as in (Woodward and Kell, 1990).

Optimal test conditions were determined by varying the concentration of suspended yeast and the driving voltage (data not shown). These experiments demonstrated that a concentration of 40 million/ml and ±2 V (peak-to-peak) was ideal for optimal signal-to-noise ratio. Increased yeast concentration gave increased variability resulting in statistically irrelevant results. Furthermore, higher voltages lead to sporadic electrode-electrolyte-interface (EEI) effects, such as hydrogen gas evolution.

NIH-PA Author Manuscript

NIH-PA Author Manuscript

NIH-PA Author Manuscript

Preliminary tests indicated interesting time-varying harmonic distortions, as measured by the setup outlined in Fig. 1, of a 1024 Hz sine wave in the presence of respiring yeast. Spectra were collected in triplicate and a representative plot of the harmonics of a respiratory-competent (Fig. 2A) and -incompetent (Fig. 2B) strain reveals that the odd harmonics correlate with respiratory capacity (rho). The third harmonic, and not higher odd harmonics, was chosen for subsequent experiments because it gave the highest signal-to-noise ratio.

In order to elaborate further on the changes in harmonics as it relates to respiration, we took a series of measurements of rho− yeast and rho+ yeast in buffers of high and low oxygen concentrations. Real-time oxygen measurements were taken with a Clark-type electrode and plotted as the percent saturation at room temperature against the elapsed time (Fig. 3A). Oxygen-saturated solutions of PBS with glucose were created by vigorous shaking. Oxygen-depleted solutions were accomplished by pulling a vacuum overnight until the start of the experiment. As indicated in Fig. 3B, the change in the third harmonic is greatest when the rho + yeast is undergoing the greatest rate of respiration as indicated by the slope of the curve in Fig. 3A. Similarly, when the rho+ yeast is placed into an oxygen-depleted solution, the change in the third harmonic is less pronounced (Fig. 3D). Please note that the delayed rise in oxygen concentration is a result of a cessation in respiration, possibly due to the Pasteur effect (Krebs, 1972) or a similar oxygen sensing mechanism. Finally, the change in the third harmonic is virtually absent in the rho− yeast (Fig. 3C). To obviate any potential bias with the spectrum analyzer, software transformation (FFT) of time records obtained from data acquisition hardware (DAQ) was used to confirm the trends in the third harmonic (data not shown).

To further validate that the third harmonic is a function of respiration, we selected a number of methods to elucidate the effects of respiratory inhibition. Rho+ yeast were treated with potassium cyanide (Fig. 4A), myxothiazol (Fig. 4B), or a mixture of antimycins (Fig. 4C) immediately before taking dielectric measurements (t=0 min.). Additionally, yeast cells were boiled for 10 min. prior (Fig. 4D). In all cases, the treatment inhibits respiration via oxygen measurements (not shown) and ablates the change in the third harmonic. Note that the maximum driving frequency was set to 3072 Hz to highlight the region of change elucidated in Fig. 3.

One obvious conclusion from Fig. 3 could be that our device is measuring changes in oxygen concentration and not any signal specific to the yeast. We pulled a partial vacuum on respiration buffer (PBS with 100 mM glucose) overnight to achieve a less than half saturated oxygen solution. The buffer was then allowed to equilibrate to maximum saturation at room temperature while harmonic measurements were taken at a range of excitation frequencies. No statistically significant changes in harmonics were seen at any of the frequencies between all oxygen concentrations (Fig. 5A). Furthermore, we wanted to rule out any effects from the mitochondrial inhibitors on the dynamics of the third harmonic spectra as it relates to Fig. 4. Fig. 5B, C, and D include third harmonic spectra at varying time points of respiration buffer with effective concentrations of inhibitors. No statistically significant differences were seen between any of the time points at each frequency measured.

Being a facultative anaerobe, S. *cerevisiae* is able to generate all of the energy requirements by fermentation alone (Altmann *et al.*, 2007). This fact makes genetic mutants, or knockout strains, lacking respiratory capacity possible and available for study from the *Saccharomyces* Genome Deletion Project. To further confirm our previous results, we took time-dependent harmonic measurements on strains lacking genes coding for a precursor protein in the electron transport chain (Fig. 6A) and a subunit of the ATP synthase complex (Fig. 6B), as well as one lacking a gene required for mitochondrial DNA maintenance (Fig. 6C). As expected, the change in the third harmonic is absent across all strains tested (oxygen data confirms respiratory incompetence).

NIH-PA Author Manuscript

NIH-PA Author Manuscript

NIH-PA Author Manuscript

4. DISCUSSION

Previous researchers (Blake-Coleman *et al.*, 1994; Woodward and Kell, 1990, 1991a, 1991b; Yositake *et al.*, 2001) have used very low frequencies (under 100 Hz) to probe the outer membrane of yeast and bacteria for enzymatic activity. The main difference between our work and previous work is our goal of probing the membranes of inner organelles using higher frequencies, namely mitochondria, for respiratory activity. Our results clearly indicate that a driving frequency of approximately 1 kHz (and not higher frequencies) correlate with temporal respiratory activity in yeast. However, it is unclear whether this frequency is sufficient to capacitively couple through the cellular membrane to excite the membranes of internal organelles since theory (Foster and Schwan, 1996; Schwan, 1957) specifies that frequencies below 1 MHz do not effectively penetrate. Woodward and Kell (1990, 1991a, 1991b), on the contrary, reported changes in harmonics as a function of respiratory capacity in the bacterium *Micrococcus luteus* at a frequency below 100 Hz, but not at 1 kHz. Since the respiratory chain of this bacterium is in its outer membrane, stimulation at 1 kHz could couple beyond the outer membrane and lead to their reported inability to detect harmonics as a function of respiratory activity at this frequency. Given an extensive, interconnected mitochondrial network (Altmann *et al.*, 2007), the simplified model used by Foster and Schwan (1996) would be insufficient to predict the frequencies capable of probing mitochondria. Thus, it appears our use of 1 kHz to probe internal membranous organelles (mitochondria) is supported by the literature as well as by our results using mitochondrial inhibitors and knockout mutants.

Another major difference between our technique and previous ones is the measurement of temporal changes in the harmonics that correlate with the measured consumption of a substrate involved in the probed enzyme(s). Using a similar experimental apparatus, Woodward and Kell (1990, 1991a, 1991b) reported only the absence or presence of harmonics of resting suspensions of microorganisms with background subtracted. Our technique serves as an extension of the previous work by recording harmonics as a function of time. Coupled with inhibition of specific cellular processes, either chemically or genetically, our technique deduced that respiratory activity in yeast correlates with temporal changes in the third harmonic. Thus, more information about the underlying biological processes can be gleaned.

Potential explanations for the correlation of increasing harmonic amplitude with respiratory activity include an increase in membrane potential that accompanies the constrained movement of respiratory chain components. The harmonics potentially arise from the unequal dipole movements of these membrane-bound proteins and their lack conformational freedom to move within the applied sinusoidal field. In addition, increased respiratory activity results in higher electron flow and membrane potentials that could lead to the observed increase in harmonic amplitudes. Theoretical work taking these factors into account has been established (Astumian and Robertson, 1989; Tsong and Astumian, 1986; Westerhoff *et al.*,1986).

Our preliminary observations with ballast resistors for dampening current fluctuations and a salt bridge for current path elimination (Schwan, 1963, 1966, see Schwan, 1992 for theoretical outline) indicate the electrode polarization region as the source for our nonlinear responses. Indeed, by removing the harmonics generated at the driving electrodes using a constant current source, Hutchings and coworkers (1994) conclude that there are no repeatable harmonics measured in the bulk. Also, in a second paper (Blake-Coleman *et al.*, 1994), the authors report reproducible harmonics unique to specific microorganisms that they attribute to the modulation of the electrode interfacial region by the presence of the cells. Our data lends support to this hypothesis that the biological material is interacting with this region to produce a modified nonlinear effect. The lack of bulk-attributable effects does not lessen the biological-relevance of this work.

NIH-PA Author Manuscript

NIH-PA Author Manuscript

NIH-PA Author Manuscript

In fact, future work in our lab aims to take advantage of the polarization region to enhance the relevant signal. Further preliminary observations indicate that bias current can be modulated using DC offset (for review see Geddes, 1997) to increase the third harmonic signal as a function of respiration. Future work will entail testing various electrode geometries and/or configurations using different materials to increase current densities in the hopes of creating a better metabolic biosensor.

5. CONCLUSIONS

In summary, this work has shown that odd harmonics resulting from the distortion of a sinusoidal electric field near 1 kHz correlate with respiratory capacity and rate in S. *cerevisiae*. Our data using respiratory-deficient mutants and mitochondrial inhibitors support the hypothesis that excitation of tissue or cells with an oscillatory electric field at certain frequencies induce conformational changes in mitochondrial membrane-bound proteins. We propose that further harmonic analysis of additional cell types, including human tissue, may lead the way for prediction of the mitochondrial bioenergetic state, including the activities of various complexes in the electron transport chain.

Acknowledgments

The authors gratefully acknowledge helpful conversations with Dale Hamilton, M.D. and William Widger, Ph.D., as well as technical assistance provided by Jie Fang. Support was provided by R21CA133153 from the National Heart, Lung, and Blood Institute and the National Cancer Institute at the NIH, the National Science Foundation, and by the ARRA supplement: 3 R21 CA133153-03S1 (NIH, NCI). Additional support was provided by the R. A. Welch Foundation (E-1221), the Texas Center for Superconductivity, and the Texas Higher Education Coordinating Board Norman Hackerman Advanced Research Program.

REFERENCES

Alberts, B.; Johnson, A.; Lewis, J.; Raff, M.; Roberts, K.; Walter, P. Molecular Biology of the Cell. 4th ed.. New York: Garland Science; 2002.

Altmann K, Durr M, Westermann B. Methods Mol. Biol 2007;372:81–90. [PubMed: 18314719]

Astumian RD, Robertson B. J. Chem. Phys 1989;91(8):4891–4901.

Bergman RN, Kim SP, Hsu IR, Catalano KJ, Chiu JD, Kabir M, Richey JM, Ader M. Am. J. Med 2007;120 (2S1):3–8.

Blake-Coleman BC, Hutchings MJ, Silley P. Biosens. Bioelectron 1994;9(3):231–242. [PubMed: 8060593]

Foster, KR.; Schwan, HP. Handbook of Biological Effects of Electromagnetic Fields. 2nd ed.. CRC Press: Boca Raton; 1996.

Geddes LA. Ann. Biomed. Eng 1997;25(1):1–14. [PubMed: 9124725]

Hutchings MJ, Blake-Coleman BC, Silley P. Biosens. Bioelectron 1994;9(2):91–103. [PubMed: 8018318]

Ingwall JS. Cardiovasc. Res 2009;81(3):412–419. [PubMed: 18987051]

Krebs HA. Essays in biochemistry 1972;8:1–32. [PubMed: 4265190]

Lowell BB, Shulman GI. Science 2005;307(5708):384–387. [PubMed: 15662004]

Neubauer S. New Engl. J. Med 2007;356(11):1140–1151. [PubMed: 17360992]

Nobrega FG, Tzagoloff A. J. Biol. Chem 1980;255(20):9821–9827. [PubMed: 6253453]

Ritov VB, Menshikova EV, He J, Ferrell RE, Goodpaster BH, Kelley DE. Diabetes 2005;54(1):8–14. [PubMed: 15616005]

Schwan HP. Adv. Biol. Med. Phys 1957;5:147–209. [PubMed: 13520431]

Schwan, HP. Determination of biological impedances. In: Nastuk, WL., editor. Physical Techniques in Biological Research. New York: Academic Press; 1963. p. 323-408.

Schwan HP. Biophysik 1966;3(2):181–201. [PubMed: 5982795]

NIH-PA Author Manuscript

NIH-PA Author Manuscript

NIH-PA Author Manuscript

Schwan HP. Ann. Biomed. Eng 1992;20(3):269–288. [PubMed: 1443824]

Sherman F. Genetics 1963;48:375–385. [PubMed: 13977171]

Sherman F, Slonimski PP. Biochimica et Biophysica Acta 1964;90:1–15. [PubMed: 14201165]

Tsong TY, Astumian RD. Bioelectrochem. Bioenerget 1986;15(3):457–476.

Westerhoff HV, Tsong TY, Chock PB, Chen YD, Astumian RD. Proc. Natl. Acad. Sci. USA 1986;83 (13):4734–4738. [PubMed: 2941758]

Woodward AM, Kell DB. Bioelectrochem. Bioenerget 1990;24(2):83–100.

Woodward AM, Kell DB. FEMS Microbiol. Lett 1991a;68(1):91–95. [PubMed: 1837530]

Woodward AM, Kell DB. Bioelectrochem. Bioenerget 1991b;26(3):423–439.

Yositake H, Muraji M, Tsujimoto H, Tatebe W. J. Electroanal. Chem 2001;496(1–2):148–152.

NIH-PA Author Manuscript
NIH-PA Author Manuscript
NIH-PA Author Manuscript

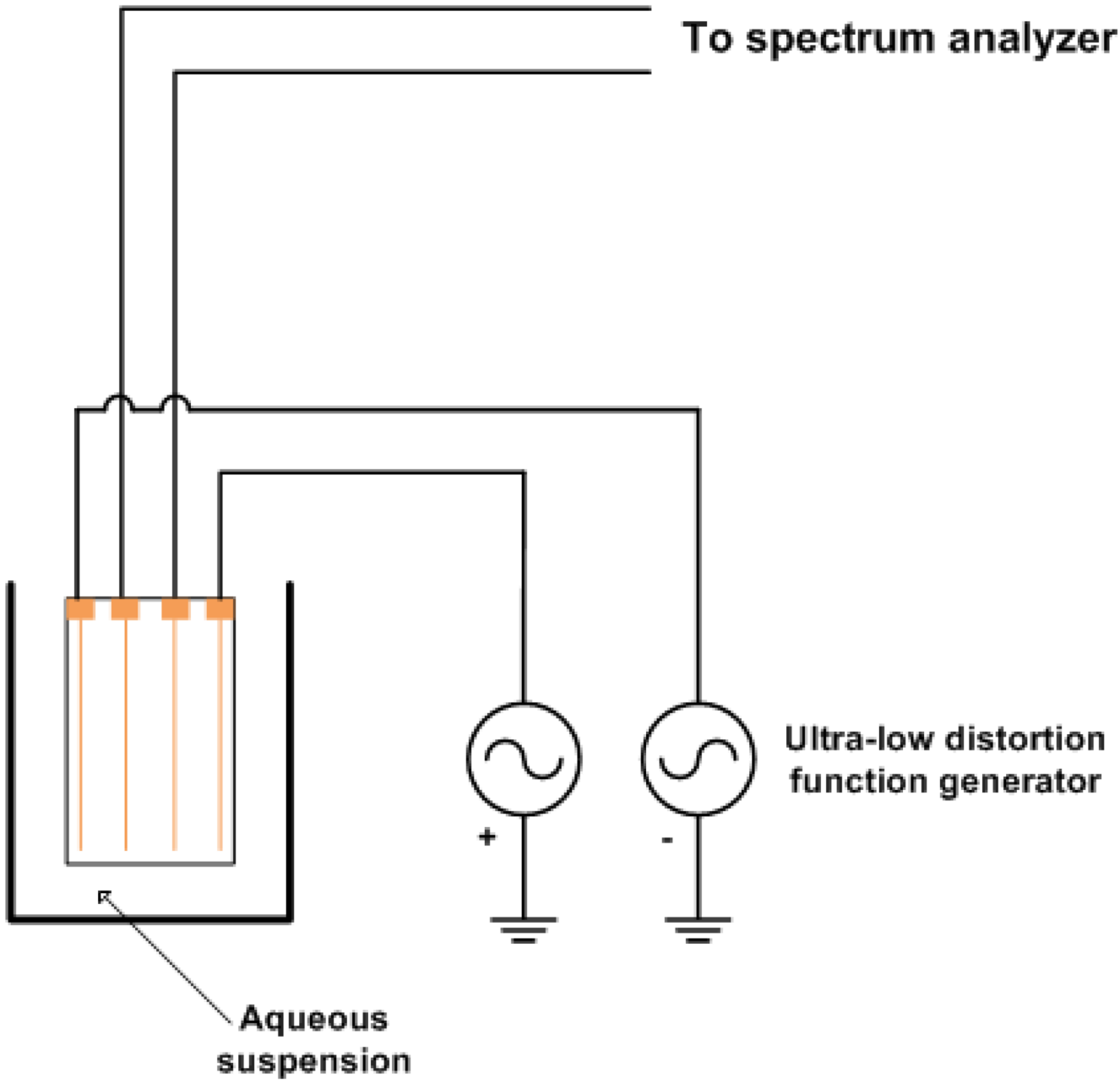

Figure 1.
Schematic showing sample holder and 4-probe gold electrode configuration. Outer electrodes were connected to the ± outputs of an ultra-low distortion function generator and the two inner wires were connected to a spectrum analyzer capable of computing the fast Fourier transform. Yeast cells were suspended by vigorous stirring during harmonic measurements.

NIH-PA Author Manuscript
NIH-PA Author Manuscript
NIH-PA Author Manuscript

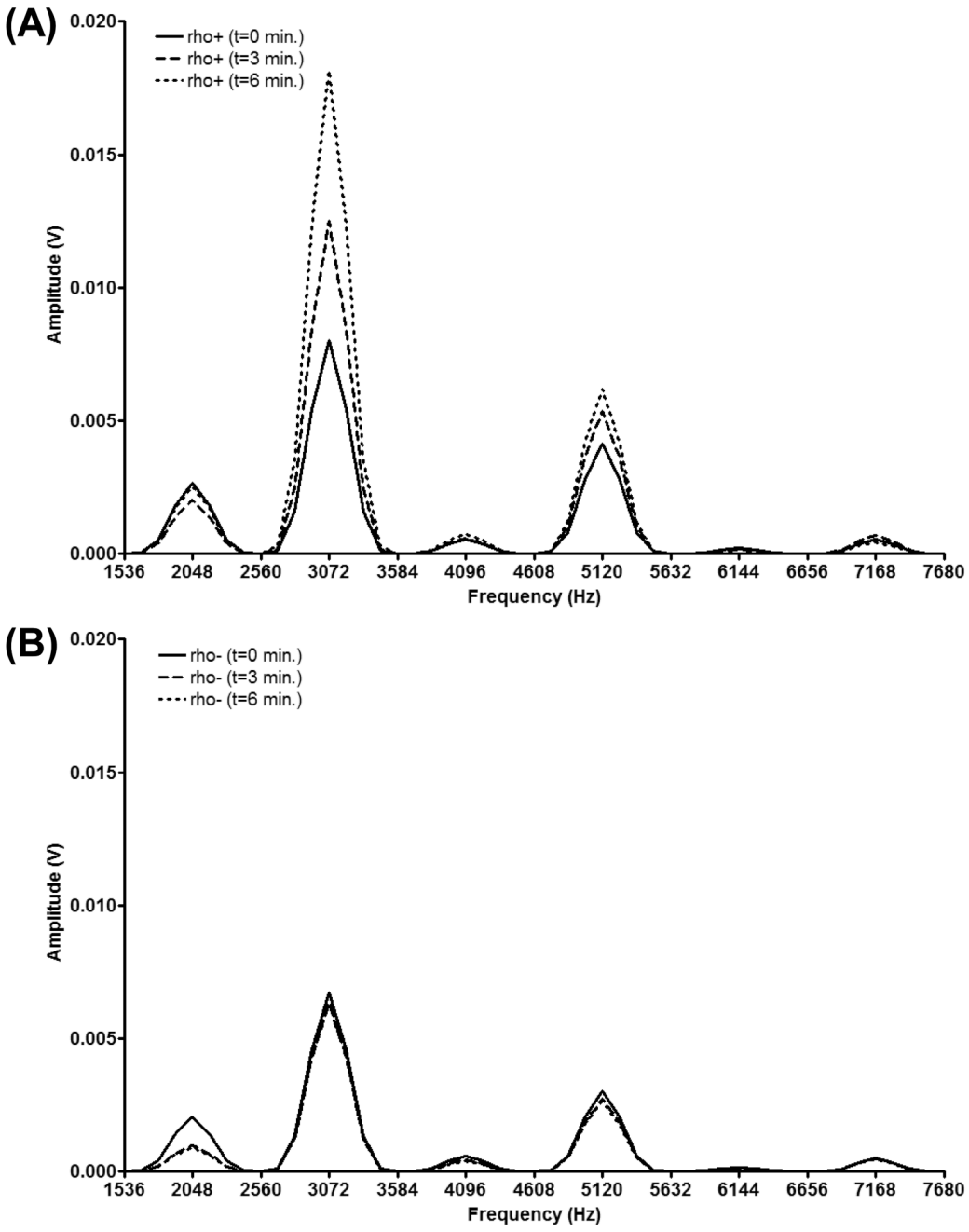

Figure 2.

Odd harmonics correlate with respiratory capacity at a driving frequency of 1024 Hz. Entire frequency spectrums were collected at 3-min. intervals upon loading the sample chamber with either respiration-competent D273-10B (A) or -deficient DS400/A12 (B) yeast strains in the presence of glucose. One representative plot out of three with the fundamental response and the higher harmonics removed is shown for clarity.

NIH-PA Author Manuscript
NIH-PA Author Manuscript
NIH-PA Author Manuscript

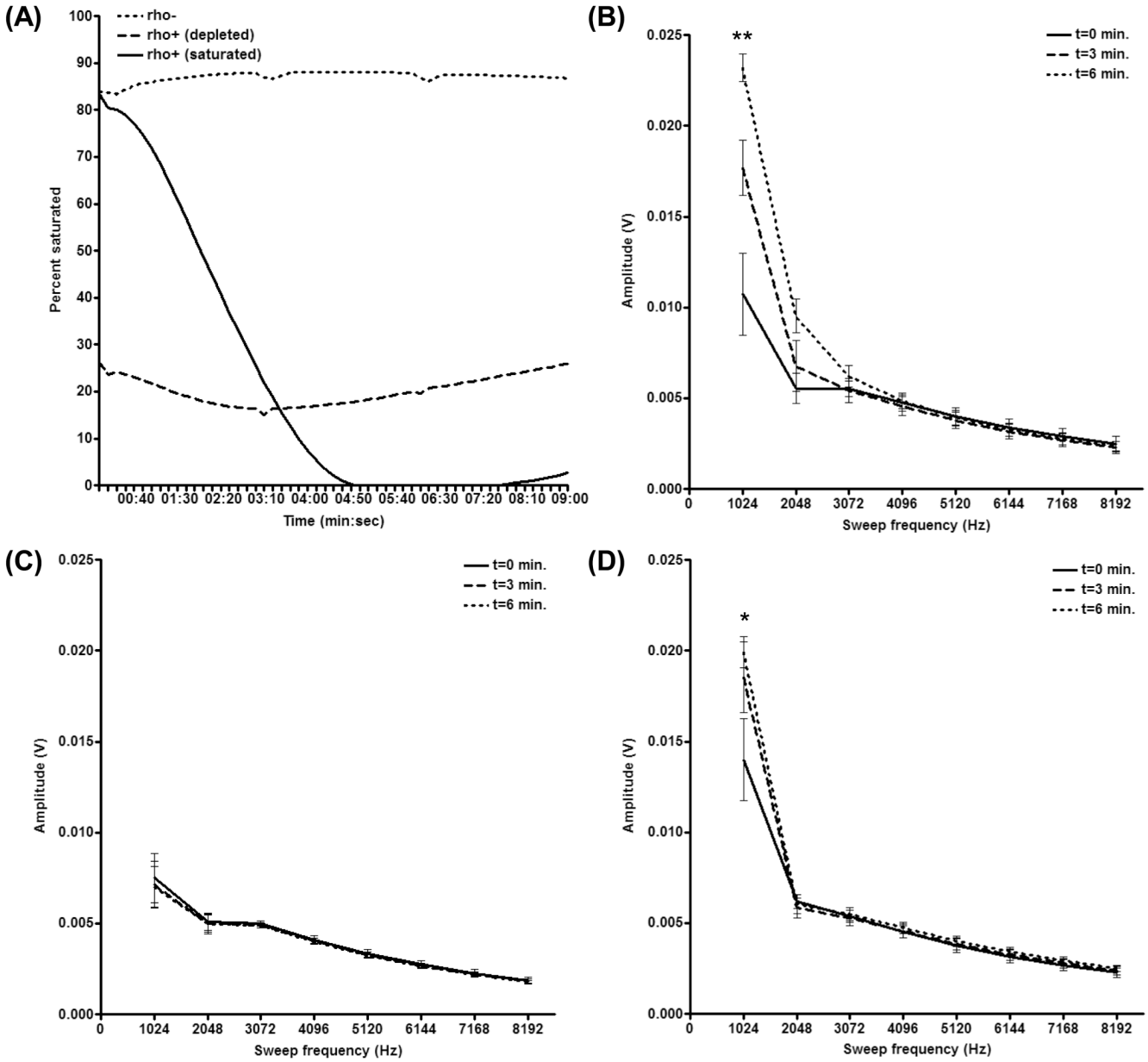

Figure 3.

Respiratory capacity and rate correlate with change in the third harmonic at low frequencies. Oxygen consumption measurements are indicated as the percent saturated at room temperature (A). The third harmonic amplitude as a function of driving frequency was taken at indicated time intervals for respiration-competent (rho+) D273-10B yeast (B) and for respiration-deficient (rho−) DS400/A12 yeast (C) placed in O_2-saturated glucose solutions. Alternatively, the rho+ yeast was placed in O_2-depleted glucose solution (D). Note the lack of temporal change in third harmonic for the rho− yeast. Experiments are represented as the mean of three independent measurements with error bars representing the standard deviations (**, $P < 0.05$ for t=0 and 3 min., and t=3 and 6 min.; *, $P < 0.05$ for t=0 and 3 min.).

NIH-PA Author Manuscript
NIH-PA Author Manuscript
NIH-PA Author Manuscript

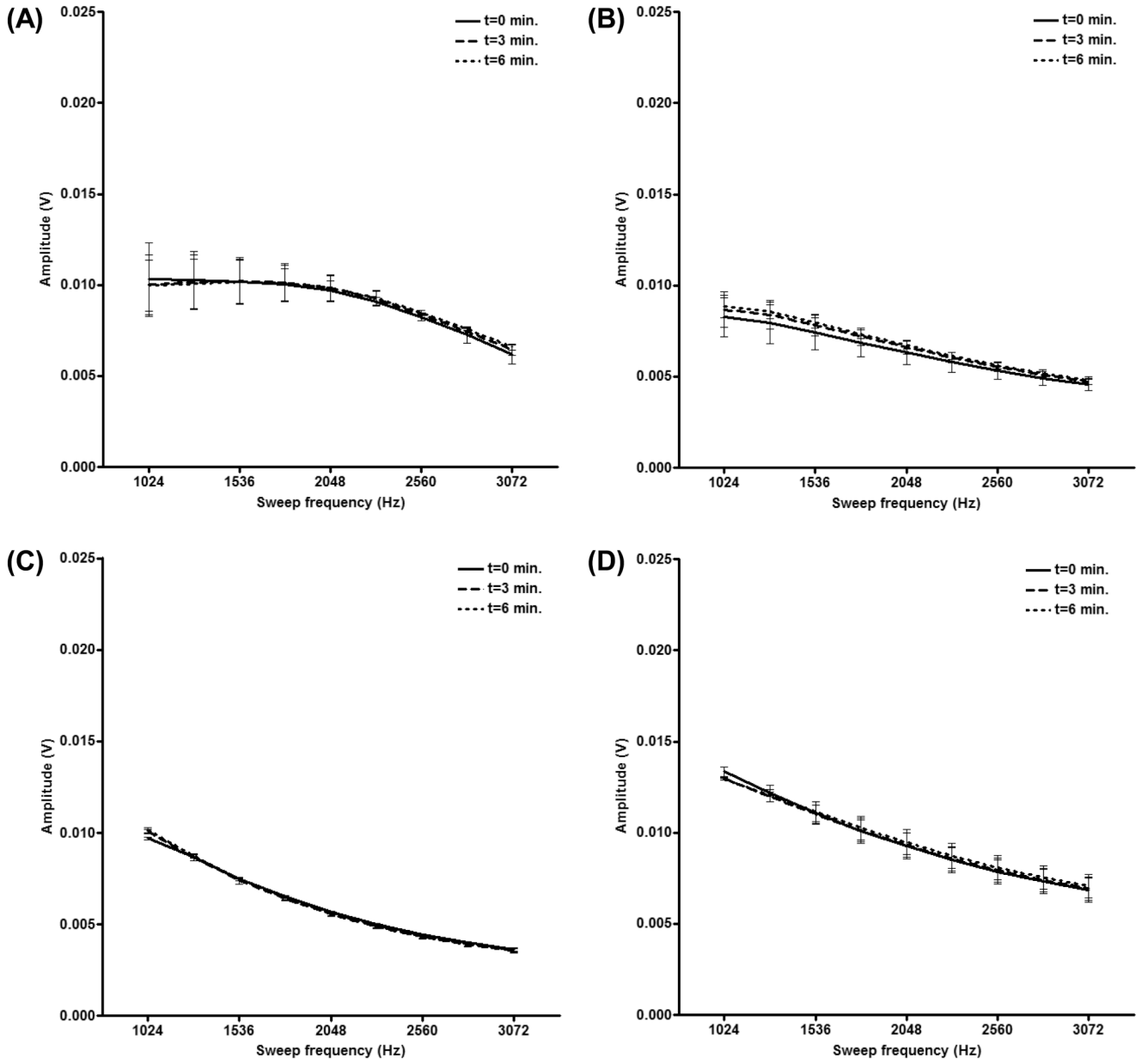

Figure 4.

Inhibition of respiration ablates change in third harmonic. Respiration-competent D273-10B strain was treated with cyanide at 200 μM (A), myxothiazol at 5 μM (B), or antimycins at ~1 μM (C) in the presence of glucose immediately before taking the third harmonic amplitudes as a function of driving frequency at indicated time intervals. Alternatively, the yeast were boiled (D) for 10 min. prior to measurement. Note that sweeps were performed at smaller increments and lower frequencies than previously as to highlight the changes seen in Fig. 3. Experiments are represented as the mean of three independent measurements with error bars representing the standard deviations.

NIH-PA Author Manuscript
NIH-PA Author Manuscript
NIH-PA Author Manuscript

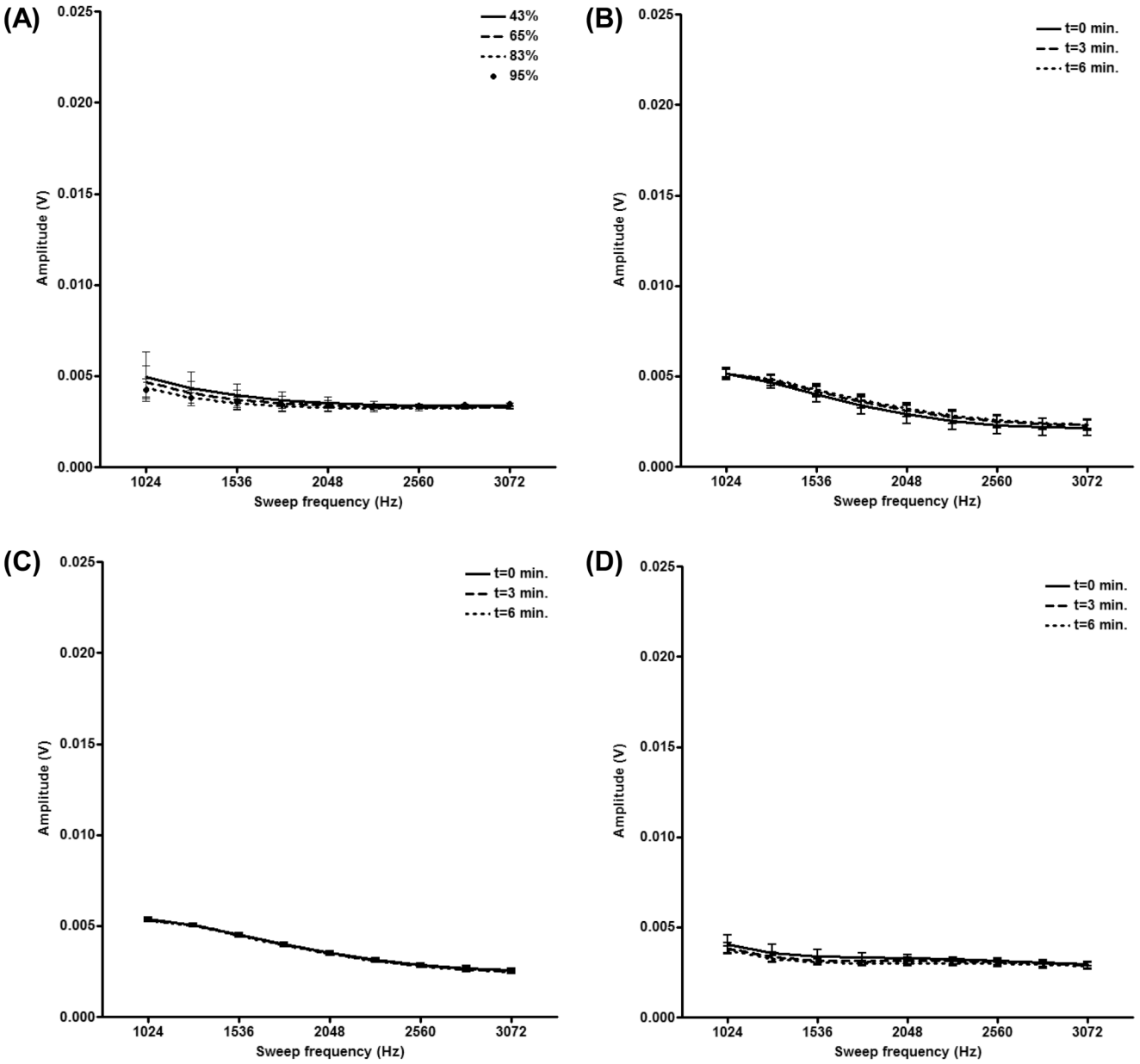

Figure 5.

Neither dissolved oxygen nor mitochondrial inhibitors affect a time-varying change on the harmonic spectra. The third harmonic amplitude as a function of driving frequency was taken of respiration buffer without yeast at indicated oxygen concentrations (A). Additionally, the third harmonic spectra were taken at indicated time intervals of respiration buffer containing 5 μM myxothiazol (B), ~1 μM antimycins (C), and 200 μM cyanide (D). Experiments are represented as the mean of three independent measurements with error bars representing the standard deviations.

NIH-PA Author Manuscript
NIH-PA Author Manuscript
NIH-PA Author Manuscript

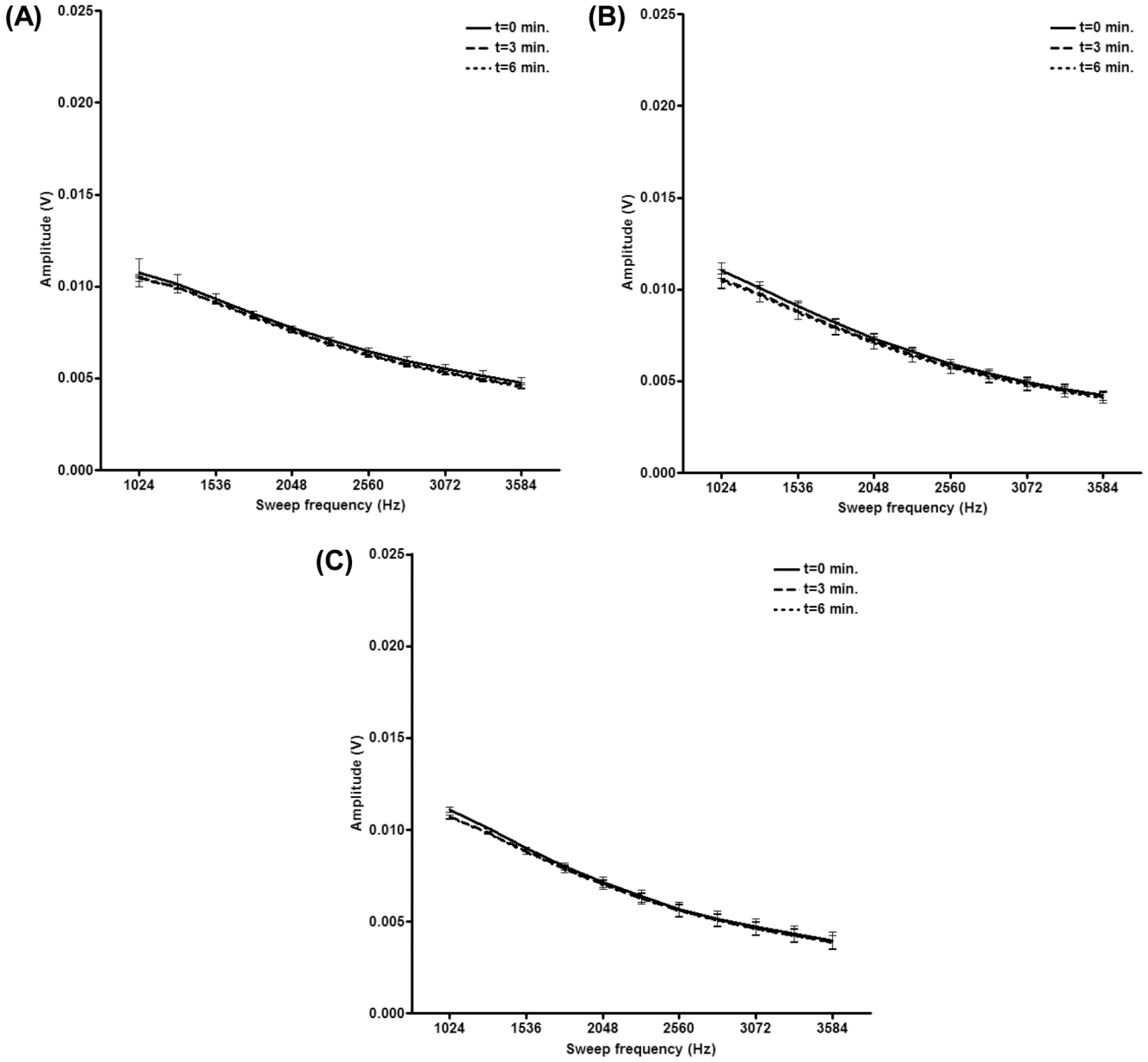

Figure 6.

Yeast knock-out mutants deficient in respiratory capacity reveal static third harmonic responses. The third harmonic amplitude as a function of driving frequency was taken at indicated time intervals for strains YEL024 (A), YBL099 (B), and YBL080 (C) in the presence of glucose. Experiments are represented as the mean of three independent measurements with error bars representing the standard deviations.